Published by
NIGERIAN SOCIETY OF PHYSICAL SCIENCES
Available online @ https://journal.nsps.org.ng/index.php/jnsps

J. Nig. Soc. Phys. Sci. 7 (2025) 2411

Journal of the Nigerian Society of Physical Sciences

A novel multi-class classification method for arrhythmias using Hankel dynamic mode decomposition and long short-term memory networks

Chuchu Liang, Majid Khan Majahar Ali*, Lili Wu

School of Mathematical Sciences, Universiti Sains Malaysia, Pulau Pinang, 11800, Malaysia

Abstract

The complex dynamic properties of ECG signals and the challenge of multi-category classification make automated diagnosis of arrhythmias difficult. In this paper, we propose a new model for the multiclassification task of arrhythmia, which combines Hankel Dynamic Modal Decomposition (HDMD) and Long Short-Term Memory Network (LSTM). HDMD is used to construct the Hankel matrix, the optimal delay parameter is selected based on 90% of the energy of the singular values, and dynamic modal features extracted from it are used as the input sequences of LSTM. The LSTM model is optimisation is performed by minimising the cross-entropy loss function, setting the maximum number of iterations to 60 and using an early stopping strategy to avoid overfitting. The model was validated on the MIT-BIH arrhythmia database, which contains 109,402 beats and is classified into five categories according to the AAMI criteria: normal beats (N), ventricular premature beats (V), fusion beats (F), atrial premature beats (S) and unclassifiable (Q). By comparing with the direct use of LSTM, the experimental results showed that the HDMD-LSTM model showed different degrees of improvement in all five classifications, especially in the classification of atrial premature beats (S) and ventricular premature beats (V), and the overall classification accuracy improved to 0.85. Future work can focus on two aspects: first, to solve the category imbalance problem, by over sampling or undersampling techniques to improve the classification ability of a few categories; second, exploring the embedding of DMD into the network structure of LSTM to further optimise the feature extraction and classification performance.

DOI:10.46481/jnsps.2025.2411

Keywords: Dynamic Mode Decomposition (DMD), Long Short-Term Memory (LSTM), Arrhythmia, Multi-Class

Article History :
Received: 03 October 2024
Received in revised form: 26 December 2024
Accepted for publication: 03 January 2025
Published: 02 March 2025

Communicated by: B. J. Falaye

1. Introduction

Arrhythmia is a common cardiovascular disease [1], which manifests itself as an abnormal frequency or rhythm of the heartbeat, which may be related to abnormal agitation of the sinus node or abnormal conduction channels, and can lead to sudden death or heart failure in severe cases [2]. With the rising incidence of cardiovascular diseases, early detection and accurate classification of arrhythmias have become crucial [3].

Electrocardiogram (ECG), as a commonly used cardiac monitoring tool, can effectively record the electrical activity of the heart and help identify arrhythmias. However, due to

*Corresponding author Tel. No: +60-149-543-405
Email address: majidkhanmajaharali@usm.my (Majid Khan Majahar Ali)

their variety and complexity, it is difficult to accurately identify them by traditional methods; therefore, automated and intelligent classification methods are important for improving diagnostic accuracy and early intervention. ECG plays a key role in arrhythmia detection and diagnosis. As a non-invasive and convenient tool, ECG records the electrical activity of the heart in real time and identifies normal and abnormal rhythms by analysing waveform features. For example, atrial premature beats are characterised by an early P-wave, while ventricular premature beats are characterised by a wide QRS wave. With prolonged monitoring techniques such as Holter, ECG can also capture episodic arrhythmias, dramatically improving diagnostic accuracy. Its widespread use not only supports early detection of arrhythmias and personalised treatment, but also provides rich data for algorithmic research.

The MIT-BIH Arrhythmia Database, a standard dataset for arrhythmia classification studies, was created by MIT in collaboration with Beth Israel Hospital and contains 48 patients' long-duration Holter-monitored ECGs. records. The database covers a wide range of arrhythmias, such as normal sinus rhythm, atrial premature beats, and ventricular premature beats, and provides detailed annotation information, making it an important benchmark for the development of ECG signal processing and automated diagnostic systems. The two-lead ECG signals in the database effectively capture the electrical activity of the heart, especially the clear R-wave signals, and facilitate the monitoring of common arrhythmias.The AAMI's five classification criteria (N, S, V, F, and Q) simplify the categorisation of arrhythmias and allow for a more consistent and objective algorithmic assessment.

Dynamic Modal Decomposition (DMD) is a technique that extracts the main modes in a dynamic system by matrix decomposition, which is able to identify the frequency, amplitude and other features of the system [4]. However, the limitations of DMD in the multiclassification arrhythmia task are also more obvious, mainly in its inability to adequately capture the nonlinearity and complexity of the data. To overcome this problem, this study introduces a long short-term memory network (LSTM) in combination with DMD, which enhances the identification of complex arrhythmia patterns by exploiting the long-term dependence modelling capability of LSTM. DMD extracts the key dynamic modes through Hankel matrix [5], while LSTM further processes these modes by selectively focusing on long-term dependence temporal features [6]. Such a combination not only improves the classification accuracy but also overcomes the shortcomings of DMD in handling multi-category tasks.

In addition, the physical interpretability of DMD enables it to reveal dynamic changes in ECG signals and provide clear pathological implications, which is not the case with many black-box deep learning models. This property allows this study not only to pursue high classification accuracy but also to support clinicians in understanding and diagnosing complex cardiac rhythm problems. In the five classification tasks of arrhythmia, the combined approach of DMD and LSTM effectively captures the subtle changes in the ECG signal and significantly improves the classification performance compared to either method alone, while maintaining the interpretability of the dynamic modalities.

In this study, we improve the ECG classification performance by combining DMD and LSTM models. Firstly, we extracted dynamic features from the ECG signal using DMD and retained the dominant modality of 90% of the singular value decomposition energy by optimising the delay parameter of the Hankel matrix. Subsequently, these features are fed into an LSTM model using an adaptive learning rate optimiser, Adam, to automatically adjust the learning rate to ensure stability and fast convergence of the training process. This combined approach enhances the DMD's ability to recognise complex arrhythmia patterns and effectively improves classification performance.

The main contributions of this study are:

- applies a combination of HDMD and LSTM to a five-classification arrhythmia task; specifically, DMD focuses on extracting spatial dynamic patterns in ECG signals, while LSTM captures important temporal correlations in the signals through its ability to model in the temporal dimension. This combination not only enhances the modal analysis of arrhythmia features, but also improves the understanding of the temporal evolution of the signal.

- the delay parameter of the Hankel matrix was optimised to improve the efficiency and stability of feature extraction by retaining the dominant mode with 90% singular value decomposition energy.

- the training stability and classification performance of the model is enhanced by using the adaptive learning rate optimiser Adam and optimising the sequence length and the number of hidden layer units of the LSTM. During the training process with a maximum iteration number of 60, the performance of the model tends to be stable in the validation set at 36 epochs.

- the validity of the proposed model was verified by evaluating it on the MIT-BIH arrhythmia database and comparing it with the direct use of LSTM.

The paper is organised as follows: section 2 reviews the traditional methods for arrhythmia classification and the current status of DMD and LSTM applications. Section 3 describes in detail the combined HDMD and LSTM approach, the optimisation process of the Hankel matrix, and the key parameter settings of the LSTM. A partial discussion in section 4 demonstrates the classification performance of the model on the dataset and provides a detailed analysis of the results. Finally, section 5 and section 6 summarises and discusses the research results, pointing out the advantages of the model and future research directions.

2. Related work

Arrhythmia classification is a key task in the analysis of ECG signals, and early studies relied on feature engineering methods using techniques such as Fourier transform

and wavelet transform to extract time, frequency and time-frequency domain features from ECG signals, such as R-wave peaks, heart rate variability (HRV), P-wave and QRS waveforms, followed by the use of machine learning, such as support vector machines (SVMs), decision trees, and K-nearest neighbours (KNN) algorithms for classification [7–13]. However, the manual feature extraction process is complex and data-dependent, and cannot cope with diverse and complex arrhythmia patterns.

With the development of deep learning, automated methods based on neural networks have gradually been applied to arrhythmia classification [14]. Convolutional neural network (CNN) performs well in ECG signal classification by automatically learning local features, but it is prone to lose timing-dependent information in the processing of non-smooth signals over long time scales [15–17]. In contrast, recurrent neural networks (RNNs) and their improved form, LSTMs, are better able to capture long-term dependent information in time-series data, and thus are more suitable for arrhythmia classification [18–21]. Despite the excellent performance of deep learning models in feature extraction and classification, the complex dynamic nature of arrhythmia is still not fully resolved, and it is a research challenge to effectively capture and extract the dynamic patterns in the signal.

HDMD combines DMD and Hankel matrix to capture multi-scale dynamic features by constructing Hankel matrix embedded in time series data [22]. DMD originated from hydrodynamic analysis and focuses on extracting dynamic modal information from time series data, and has been widely used in signal processing and time series analysis [23]. HDMD, by introducing delay embedding, has enhances the ability of DMD to capture nonlinear features, which is particularly suitable for the analysis of non-stationary ECG signals. Ingabire *et al.* [5] successfully applied DMD in biomedical signal analysis to extract key dynamic modes [5]. Although HDMD has relatively few applications in arrhythmia classification, its powerful temporal decomposition capability offers potential for ECG signal classification.

LSTM, as an improvement of RNN, solves the problem of gradient vanishing in long time-series data by introducing forgetting gate, input gate and output gate, which is well suited to deal with the long-term dependence characteristics in ECG signals. Chung *et al.* [24] proposed an arrhythmia classification method based on LSTM, and used LSTM to classify ECG signals directly with good results [24, 25]. Hou *et al.* [18] combined the LSTM with an autoencoder to further improve the performance of arrhythmia classification [18]. Although LSTM performs well in arrhythmia classification, it still relies on the quality of input features. Therefore, inputting HDMD-extracted dynamic modalities into LSTM can help improve classification accuracy and optimise overall model performance.

Existing techniques still exhibit certain limitations:

1. While many deep learning-based models excel in classification accuracy, their ‘black-box’ nature makes them less interpretable, making it difficult to provide clinicians with intuitive explanations of pathology.
2. The common category imbalance problem in arrhythmia classification tasks remains intractable, with rare abnormal rhythm categories often lacking sufficient samples for training, thus affecting the generalisation ability of the model.
3. ECG signals are usually affected by noise, baseline drift and other disturbances, and it remains a challenge to accurately extract effective features in a noisy environment.

Therefore, to address the shortcomings of DMD in multiclassification of arrhythmias, we propose a new model. By combining the physical interpretability of DMD and the time-series modelling capability of LSTM, we effectively address the challenges in ECG multiclassification. Hankel DMD extracts dynamic modalities in ECG signals to enhance the model’s interpretability and help clinicians understand the dynamics of arrhythmias, and improves the identification of rare categories by preserving 90% of the singular value energy.LSTM, on the other hand, focuses on time sequence modelling, which deals with long-term dependence and complex temporal features to effectively deal with noise and baseline drift. This improves the classification performance and robustness of the model.

3. Materials and methods

Figure 1 illustrates the general flow of the study. Firstly, the definition of the research objectives serves as a starting point to clarify the objectives of multiclassification of arrhythmias.

Then, the flowchart shifts to the data preparation stage, which involves extracting data from the MIH-BIT arrhythmia database and performing preprocessing such as beat segmentation, filtering, normalisation, and dataset partitioning. Subsequently, construction of Hankel matrix is the key step and this phase involves selecting appropriate delay parameters and performing singular value decomposition to optimise the model. DMD follows and is applied to the Hankel matrix to extract dynamic features. The extracted features are then fed into the LSTM model for training and classification. Finally, the classification performance is analysed and model tuning is performed through a model evaluation and optimisation phase to ensure the best results. The final part of the flowchart summarises the result analysis, outlining the main findings and conclusions of the study.

3.1. ECG dataset

The MIH-BIT arrhythmia database used in this paper contains multiple types of arrhythmia ECG data [26], a total of 48 ambulatory ECG recordings of approximately half an hour’s duration from 47 patients (records 201 and 202 are from the same patient), sampled at a frequency of 360 Hz. The database was created by the Massachusetts Institute of Technology (MIT) and Beth Israel Hospital between 1975 and 1979 and covers over 4000 Holter records, 60% inpatient and 40% outpatient. The database contains 15 beat types, totalling approximately 109,402 beats, of which approximately 70% are normal beats and 30% are abnormal beats (e.g., atrial premature beats, ventricular premature beats, atrial fibrillation, etc.). For

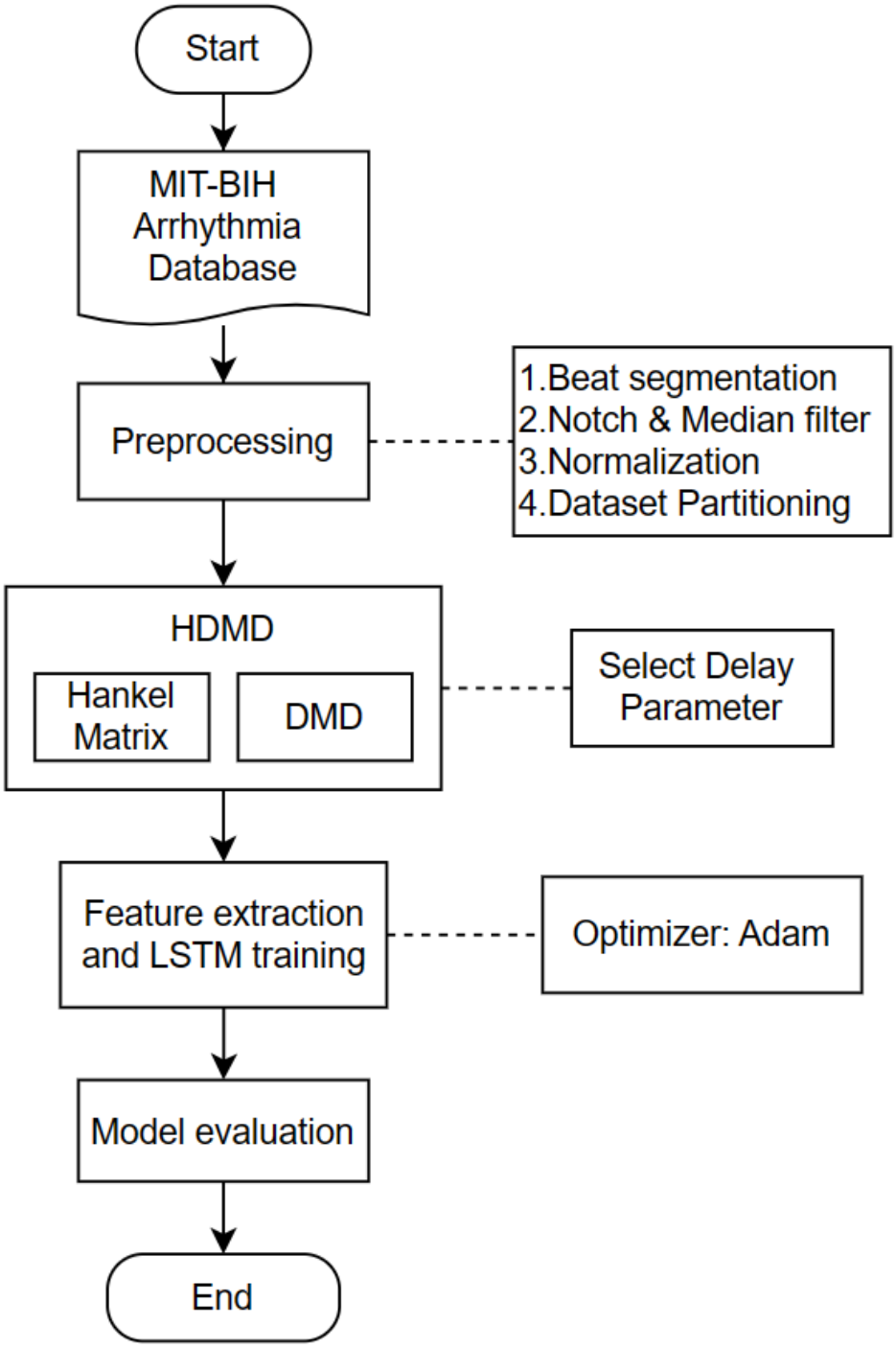

Figure 1. A general overview diagram of the method.

detailed information, see Table 1. Each ECG record contains 2 leads, with 45 records using the corrected Limb II lead as the first lead and the remaining records using the V5 lead, and 40 records using the corrected V1 lead as the second lead and the remaining records using the V2, V4, or V5 lead. Each record consisted of a header file, a data file, and an annotation file, with the annotation file being provided by at least two ECG specialists, and included the QRS main wave position, lead information, ECG signal storage format, sampling frequency, beat type, rhythm, arrhythmia position, and patient information.

3.2. *Data preprocessing*

First, beat segmentation was performed to extract the heart beat cycle. Using annotation files from the MIT-BIH arrhyth-

Table 1. Heart beat information in the MIT-BIH arrhythmia database

Class	Beat type	Abbreviation	Total
N	Normal beat	NOR	75011
	Left bundle branch block beat	LBBB	8072
	Right bundle branch block beat	RBBB	7255
	Atrial escape beat	AE	14
	Nodal (Junctional) escape beat	NE	206
V	Premature ventricular contraction	PVC	7129
	Ventricular escape beat	VE	106
F	Fusion of ventricular and normal beat	FVN	802
S	Atrial premature beat	AP	2540
	Aberrated atrial premature beat	aAP	148
	Nodal (Junctional) premature beat	NP	82
	Supraventricular premature beat	SP	2
Q	Paced beat	P	7025
	Fusion of paced and normal beat	FPN	981
	Unclassified beat	U	29
Total			109402

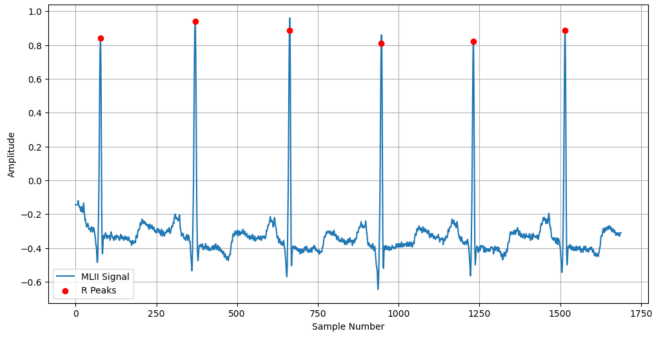

Figure 2. R wave position marker.

mia database, we segmented the raw ECG signals into individual heart beats based on the location of QRS wave clusters. The main goal of this step is to divide long ECG signals into segments of heart beats with the same duration for further analysis of each heart beat. In this study, this was done first by extracting the recordings of the R-point location in the annotation file, and then selecting 175 sampling points from each side of the R-point, for a total of 351 sampling points, which is sufficient to cover the range of the P-QRS-T wave. Figure 2. demonstrates the ECG signal segmentation for the first six R-waves. In Figure 2, the position of each R-wave is marked with a red dot to clearly highlight the exact position of the R-wave.

After data segmentation, ECG segments usually contain high-frequency noise and power-frequency disturbances (e.g., 50 Hz industrial frequency noise). In order to eliminate these noises and improve the signal quality, we perform a two-step filtering process on the signal: notch filtering and median filtering.

1. Notch filtering: removal of power disturbances is followed by low-pass filtering to remove high-frequency noise. Trap filtering is mainly used to remove interference signals at specific frequencies, here Infinite Impulse Response (IIR) filter is used [27].

$$x_n = y_n - a_1 x_{n-1} - a_2 x_{n-2}, \tag{1}$$

where y_n is the input ECG signal, x_n is the filtered ECG signal, and a_1 and a_2 are the coefficients of the filter, which are determined according to the centre frequency and bandwidth of the notch filter.

2. Median filtering [28]: by taking the median value of the data within the filtering window instead of the value of the current data point, the noise in the signal can be effectively removed, taking into account the effect of denoising while retaining a clearer signal. There is a signal x_n to be filtered, set the length of the window as L, the filtered signal is $\hat{x}_n$. For the i-th data point, select a window of length L containing the i-th data point, sort the L data points in the window from smallest to largest, and then take the middle value as the filtering result of the i-th data point:

$$\hat{x}_i = M\left(x_{i-\frac{L-1}{2}}, x_{i-\frac{L-1}{2}+1}, \ldots, x_{i+\frac{L-1}{2}}\right), \tag{2}$$

where M denotes the median-taking operation. $i \in (\frac{L-1}{2}, N-\frac{L-1}{2})$ and N is the data length. When the window L = 1, the median filter degenerates to the case where no filtering is performed, i.e., $\hat{x}_n = x_n$.

In the process of ECG signal acquisition, the accuracy of ECG signal acquisition is not affected by the potential size and position of the sensor, however, due to the relationship between the distance between the reference point and the R-wave in different ECG cycles of the same person, i.e., the distance between them varies with the change of the heart rate, for this reason, it is necessary to normalise the ECG cycle to eliminate the amplitude difference between different patients, so that the reference point can effectively represent the relative position within a cycle. relative position within a cycle. The normalisation process for each ECG sample x is shown by the following equation:

$$X^* = \frac{x - x_{\min}}{x_{\max} - x_{\min}}. \tag{3}$$

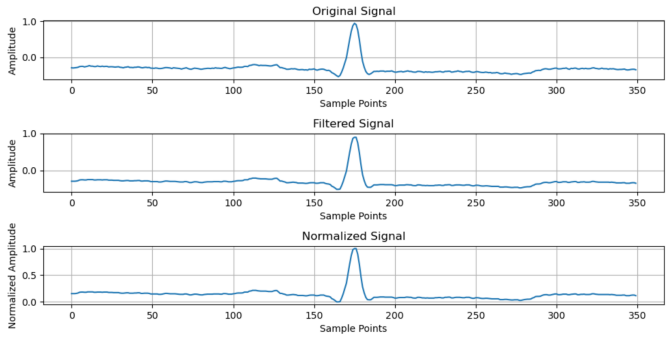

Figure 3. ECG signal processing example: original, filtered, and normalized signal.

Table 2. Dataset 1 (DS1) and dataset 2 (DS2) from the MIT-BIH arrhythmia database. Heartbeat type and class abbreviations are defined in Table 1.

Class	Beat type	DS1	Total	DS2	Total
N	NOR	38101	45862	36410	44196
	LBBB	3948		4124	
	RBBB	3783		3472	
	AE	14		0	
	NE	16		190	
V	PVC	3682	3787	3220	3221
	VE	105		1	
F	FVN	415	415	387	387
S	AP	806	938	1734	1834
	aAP	98		50	
	NP	32		50	
	SP	2		0	
Q	P	0	8	0	6
	FPN	0		0	
	U	8		6	
Total			51010		49644

In Eq. (3), xmin denotes the minimum value of ECG sample amplitude and xmax denotes the maximum value of ECG sample amplitude. All normalised ECG samples have a common feature that all their amplitudes are greater than 0 and less than 1. Figure 3 shows the three steps of ECG signal processing. The first subfigure shows the original ECG signal; the second subfigure shows the filtered signal with noise and interference removed; and the third subfigure presents the normalised signal with all amplitudes united to the [0, 1] range. These processing steps improve the quality and consistency of the signal and prepare it for further analysis.

ECG beats were categorised according to the AAMI (Association for the Advancement of Medical Instrumentation) standards.The original markers in the MIT-BIH database contain 15 ECG beat types. In order to be more relevant to practical clinical applications and basic patient assessment, we reclassified these beats into five main categories: normal beats (N), supraventricular ectopic beats (S), ventricular ectopic beats (V), fusion beats (F), and ventricular ectopic beats (V). , fusion beats (Fusion beats, F), and unclassified beats (Unclassified beats, Q). This classification simplifies the classification task of the model and complies with common standards in the medical field. In this paper, the standard dataset division method defined in the study of de Chazal *et al.* [29] was used to divide the records in the MIT-BIH arrhythmia database into a training set DS1 and a test set DS2. The specific divisions are as follows:

The training set DS1 contains the following records: 101, 106, 108, 109, 112, 114, 115, 116, 118, 119, 122, 124, 201, 203, 205, 207, 208, 209, 215, 220, 223, 230

The test set DS2 contains the following records: 100, 103, 105, 111, 113, 117, 121, 123, 200, 202, 210, 212, 213, 214, 219, 221, 222, 228, 231, 232, 233, 234. 102, 104, 107, 217 not included in DS1 and DS2.

Table 2 shows the distribution of the various beat types in the MIT-BIH arrhythmia database, with data from DS1 and DS2, and lists the number of beats of each beat type in both datasets, as well as the total number of beats in each of the five categories, with the number of training samples being 51,010, and the number of test samples being 49,644.

3.3. Hankel dynamic mode decomposition

3.3.1. Construct Hankel matrix

ECG signal data for individual beats were extracted from the MIH-BIT arrhythmia database. Each beat signal consists of $N = 2$ leads, and after preprocessing, each lead contains $T = 351$ sampling points. The ECG data collected from N leads at time t, is denoted as $x_t \in R^N, t = 1, \cdots, T$ and the whole dataset is represented as:

$$X_T = \begin{pmatrix} x_{1,1} & \cdots & x_{1,351} \\ x_{2,1} & \cdots & x_{2,351} \end{pmatrix} = [x_1, \ldots, x_t, \ldots, x_T] \tag{4}$$

Next, a Hankel matrix H was constructed to expand the dimensionality of the data to solve the rank mismatch problem (i.e., $2 << 351$). Given a delayed embedding length M, we can construct H from X by a Hankelization operation. For each row of X_T, i.e., the ECG signal data on each lead of the patient, the corresponding Hankel matrix is constructed as follows:

$$H_1^n = \begin{pmatrix} x_{n,1} & x_{n,2} & \cdots & x_{n,T-M+1} \\ x_{n,2} & x_{n,3} & \cdots & x_{n,T-M+2} \\ \vdots & \vdots & \ddots & \vdots \\ x_{n,M} & x_{n,M+1} & \cdots & x_{n,T} \end{pmatrix}^T_{M\times(T-M+1)} \tag{5}$$

$$H_2^n = \begin{pmatrix} x_{n,2} & x_{n,3} & \cdots & x_{n,T-M+2} \\ x_{n,3} & x_{n,4} & \cdots & x_{n,T-M+3} \\ \vdots & \vdots & \ddots & \vdots \\ x_{n,M+1} & x_{n,M+2} & \cdots & x_{n,T+1} \end{pmatrix}^T_{M\times(T-M+1)} \tag{6}$$

We can get $H_2^n = A_H H_1^n$, and rearrange the Hankel matrices on each lead to get a new matrix:

$$H_1 = (H_1^1, H_1^2)^T \in R^{2M\times(T-M+1)}, \tag{7}$$

$$H_2 = (H_2^1, H_2^2)^T \in R^{2M\times(T-M+1)}. \tag{8}$$

In this way, H_1 and H_2 are used as inputs to the DMD, so that the DMD modal extraction problem becomes a search for

eigenvalues and eigenvectors with respect to AH in the following equation [30].

$$H_2 = A_H H_1. \tag{9}$$

The construction of the Hankel matrix aims at capturing the dynamic features of the time series data and transforming them into a high-dimensional matrix. After completing the construction of the Hankel matrix, we apply the DMD for analysis.The main objective of the DMD is to find a low-rank representation in order to reconstruct the time series approximately by a linear combination of dynamic modes.

Algorithm 1: Hankel DMD

- Apply Singular Value Decomposition (SVD): $H_1 = U\Sigma V^*$
- Calculate an alternative representation of A_H: $A_H = H_2 V \Sigma^{-1} U^*$
- Compute $\tilde{A}_H$: $\tilde{A}_H = U_r^* A_H U_r$, $\tilde{A}_H = U_r^* A_H V_r \Sigma_r^{-1}$
- Compute the relative energy R_i: $R_i = \frac{\sum_{j=1}^{r_i} \sigma_j}{\sum_{j=1}^{MN} \sigma_j}$ (i=1,2,. . .,max)
- Extract dynamic modes:
- Solve for eigenvalues and eigenvectors: $\tilde{A}_H W = W\Lambda$
- Calculate dynamic modes: $\Phi_H = H_2 V \Sigma^{-1} W$
- Reconstruct the signal, Compute $\hat{H}$: $\hat{H} = \sum_{k=1}^{r} \phi_k e^{\omega_k t} b_k$
- Define a dictionary M to store all modes extracted by HDMD
- Loop through each ECG sample:
- for i in range(ECG sample size) do
- Extract the sample signal and process it
- Construct the Hankel matrix and perform DMD decomposition
- Store the extracted modes in dictionary M: $M[i]$ = extracted modes
- end for
- Output: Set of dynamic features $\{\Phi_H, \hat{H}\}$ and mode dictionary M
- End

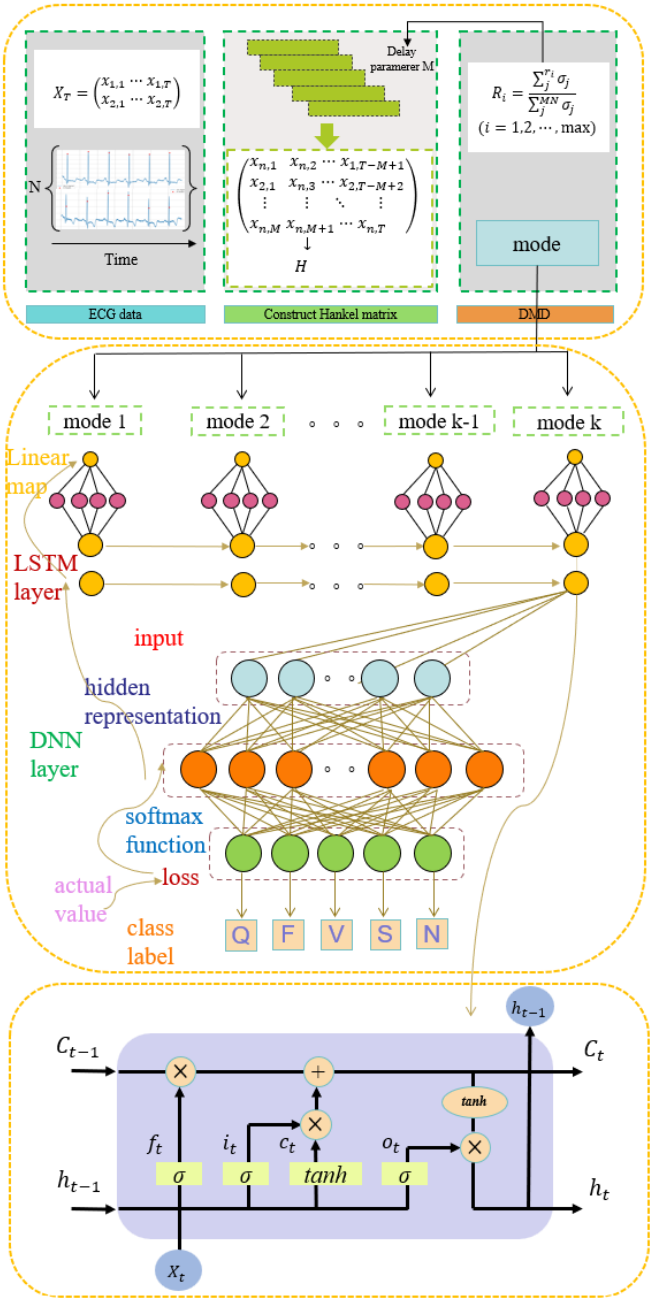

Figure 4. HDMD-LSTM ECG Arrhythmias multi-classification model framework.

3.4. LSTM network architecture

LSTM network is a neural network specially designed to process temporal data. In this paper, the dynamic modalities extracted by HDMD are input as features into the LSTM network for arrhythmia classification.The basic structure of LSTM includes input gates, forgetting gates, and output gates, which deal with long-time dependencies by controlling the flow of information, and the structure of the model is shown in Figure 4.

Input representation:

for each input signal fragment, we extract k dynamic modes $\{\phi_1, \phi_2, \cdots, \phi_k\}$ by HDMD, and let each mode ϕ_i be a vector:

$$\phi_i = \{\phi_{i,1}, \phi_{i,2}, \ldots, \phi_{i,n}\}, \tag{10}$$

where n is the length of the modality, i.e., the number of elements contained in that modality. These extracted dynamic modes ϕ_i will be used as inputs to the LSTM. For the LSTM, the input is a sequence that receives a complete vector of modalities $\phi_t = \phi_i$ at each time step t. Therefore, the LSTM will sequentially receive $\phi_1, \phi_2, \cdots, \phi_k$ as input sequences at time step $t = 1, 2, \cdots, k$. The shape of the input data is '(batch_size, k, n)', where k is the sequence length and n is the input dimension.

Forget Gate:

The forget gate determines how much previous information is discarded. The formula is:

$$f_t = \sigma(W_f \cdot [h_{t-1}, \phi_t] + b_f), \tag{11}$$

where f_t is the output of the forgetting gate, taking values between [0,1], which indicates how much of the previous state is forgotten. W_f and b_f are weight matrices and bias terms, h_{t-1} is the hidden state of the previous moment, ϕ_t is the modal state of the current input, and σ is the sigmoid activation function, which is used to control the amount of information flow through, and whose output value is between [0,1].

Input Gate:

the input gate determines the importance of the current information and calculates the new information that is currently to be added to the cell state. The formula is as follows:

$$i_t = \sigma(W_i \cdot [h_{t-1}, \phi_t] + b_i). \tag{12}$$

Candidate cell status update:

$$\tilde{C}_t = \tanh(W_C \cdot [h_{t-1}, \phi_t] + b_C), \tag{13}$$

where *tanh* is used for state updating as it has a range of output values of [-1,1] which better expresses state changes.

Cell state update:

The LSTM cell updates the past state and new input information. The update formula is as follows:

$$C_t = f_t * C_{t-1} + i_t * \tilde{C}_t, \tag{14}$$

where C_t is the cell state at the current moment, which is used to store information for long-term memory, and C_{t-1} is the cell state at the previous moment.

Output Gate:

The output gate determines what hidden state is output at the current moment. The formula is:

$$o_t = \sigma(W_o \cdot [h_{t-1}, \phi_t] + b_o). \tag{15}$$

Hidden state update:

The output of the LSTM, i.e., the final hidden state h_t incorporates information about the cell state:

$$h_t = o_t * \tanh(C_t), \tag{16}$$

where h_t is the output of the current timestep, passed to the next timestep and used for the output of the current timestep.

During training, the parameters of the LSTM are optimised by minimising the cross-entropy loss function:

$$L = -\sum_{i=1}^{N} y_i \log(\hat{y}_i), \tag{17}$$

where y_i is the true label, $\hat{y}_i$ is the probability predicted by the model, and N is the total number of samples.

During the optimisation process, we choose the Adam optimisation algorithm to update the model parameters.The Adam optimiser combines the advantages of momentum and RMSProp optimisation, and is able to adaptively adjust the learning rate of each parameter to speed up convergence and improve model performance. The learning rate is set to 0.001. During the training process, we set the maximum number of iterations (epochs) to 60, and adopt an early stopping strategy to terminate the training when the loss of the validation set is no longer decreasing in 5 consecutive iterations to avoid overfitting. The batch size is set to 32, a smaller batch size allows the model to update the parameters more frequently, which improves the convergence speed of the model and also increases the regularisation effect of the model to some extent. The way the dataset is divided has been described in detail in the preprocessing section, and model training and evaluation are performed based on these divisions during the training phase.

3.5. Evaluation metrics

In order to verify that HDMD is more accurate and effective than general DMD modal extraction, the extracted modal data and reconstructed data are classified by combining LSTM. After pre-processing such as filtering, DMD and HDMD are performed for modal extraction and reconstructed data,compare Reconstruction Mean Squared Error (MSE) [31]:

$$\text{MSE} = \frac{1}{N}\sum_{n=1}^{N} \|X_n - \hat{X}_n\|, \tag{18}$$

where $\|\cdot\|$ denotes Euclidean norm.

After model training is complete, we need to evaluate the performance of the LSTM model to ensure that it can accurately classify arrhythmias. In order to comprehensively assess the classification performance of the model, we used a 5-category confusion matrix, where we used five categories for the multi-classification task of arrhythmia and simplified them by numerical coding into the form of labelling from 1 to 5, with the following mapping relationships: 1 denotes category N (normal beats), 2 denotes category V (premature ventricular beats), 3 denotes category S (premature atrial beats), 4 denotes category F (fused beats), and 5 denotes category Q (unclassifiable). As shown in Table 3, the rows of the confusion matrix represent

Table 3. Confusion matrix for multi classification.

True label	Predicted Label					
	Class	N	V	S	F	Q
	N	M_{11}	M_{12}	M_{13}	M_{14}	M_{15}
	V	M_{21}	M_{22}	M_{23}	M_{24}	M_{25}
	S	M_{31}	M_{32}	M_{33}	M_{34}	M_{35}
	F	M_{41}	M_{42}	M_{43}	M_{44}	M_{45}
	Q	M_{51}	M_{52}	M_{53}	M_{54}	M_{55}

the actual categories and the columns represent the categories predicted by the model. We use the following shorthand to represent the elements in the confusion matrix:

In the matrix, M_{11} denotes the number of samples whose true category is N (normal beats) and are correctly classified as N. M_{12} denotes the number of samples whose true category is N (normal beats) but are incorrectly classified as V (premature ventricular beats). By analogy, each $M_{ij}(i, j = 1, 2, \cdots, 5)$ in the confusion matrix denotes the number of samples whose true category is i, but which are classified as j. Four common evaluation metrics are used in this paper: Accuracy (A), Precision (P), Recall (R) and F1-score (F1). The specific formulae for each category are as follows:

$$A = \frac{\sum_{i=1}^{5} M_{ii}}{\sum_{i=1}^{5}\sum_{j=1}^{5} M_{ij}} \times 100\%, \tag{19}$$

$$P_i = \frac{M_{ii}}{\sum_{j=1}^{5} M_{ji}} \times 100\%, \tag{20}$$

$$R_i = \frac{M_{ii}}{\sum_{j=1}^{5} M_{ij}} \times 100\%, \tag{21}$$

$$F_{1i} = \frac{2 \times (P_i \times R_i)}{P_i + R_i}. \tag{22}$$

When dealing with datasets with unbalanced categories, weighted evaluation metrics provide a fairer representation of model performance. Weighted Precision and Weighted Recall provide a comprehensive performance assessment by weighting the precision and recall for each category. The Weighted F1 Score combines the weighted results of Precision and Recall to provide a comprehensive picture of the model's performance for all categories. These weighting metrics help ensure that the predictive effectiveness of a few categories is not overlooked, thus providing a fairer assessment of performance. The specific formula is as follows,where N_i denotes the number of samples per category:

$$P = \frac{\sum_{i=1}^{5}(N_i \times P_i)}{\sum_{i=1}^{5} N_i}, \tag{23}$$

$$R = \frac{\sum_{i=1}^{5}(N_i \times R_i)}{\sum_{i=1}^{5} N_i}, \tag{24}$$

$$F_1 = \frac{\sum_{i=1}^{5}(N_i \times F_{1i})}{\sum_{i=1}^{5} N_i}. \tag{25}$$

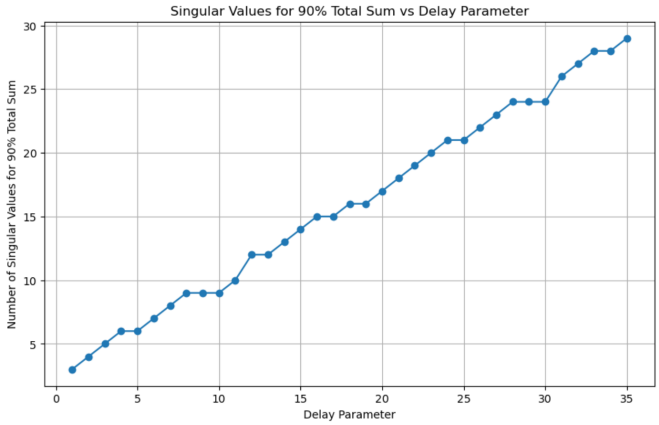

Figure 5. 90% Singular Value Ratio vs. Delay Parameter.

4. Experiment results

4.1. Experimental setup

The experiments in this paper use ECG signal data from the MIH-BIT arrhythmia database for a total of 48 patients. All experiments are performed in Python environment, data processing is performed using WFDB library for ECG signal reading and processing, and BioSPPy library for R-wave peak detection.LSTM model implementation and training are performed using TensorFlow/Keras libraries, and dataset partitioning and performance evaluation are done by scikit-learn library. The experiments were conducted on Windows 11 Pro 64-bit operating system with configurations including an Intel Core i7-10750H processor (2.60 GHz, 6 cores and 12 threads), 16 GB of RAM and 512 GB of SSD storage. The software environment includes Python 3.8, WFDB 3.1.0, BioSPPy 0.5.0, TensorFlow 2.9.0 and scikit-learn 1.1.0.

4.2. Delay parameter selection

In selecting the delay parameters for the Hankel matrix, we set up an iterative process to determine the optimal delay parameter M. The maximum delay parameter is set to max and iterated over the range from 1 to max. For an ECG signal with a data size of $(2, 351)$, the corresponding Hankel matrix has a size of $(2M, 352-M)$. To reduce the computational complexity, we chose the range of M to ensure that $2M < (352 - M)/2$.

At each iteration, we perform a singular value decomposition (SVD) of the Hankel matrix and record the delay parameter M when the singular value energy reaches 90%.Ultimately, the experimental results show that the delay parameter M is chosen to be 33, at which point the singular value energy of the Hankel matrix reaches 90% retention. This choice ensures that the main dynamic information can be fully retained during the dynamic mode extraction process, while possible noise and redundant information are filtered out. As Figure 5 illustrates the variation curve of the number r_i when the singular value ratio reaches 90% for different delay parameters.

With this delay parameter, we extracted 28 dynamic modes. This shows that while maintaining 90% of the singular value energy, we obtained 28 major modes, with the distribution of

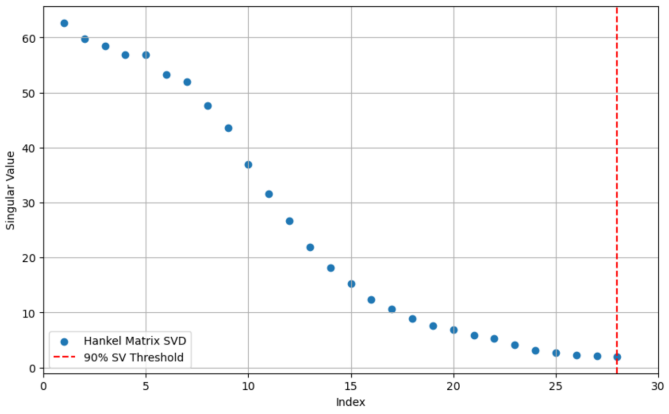

Figure 6. Singular value scatter plot.

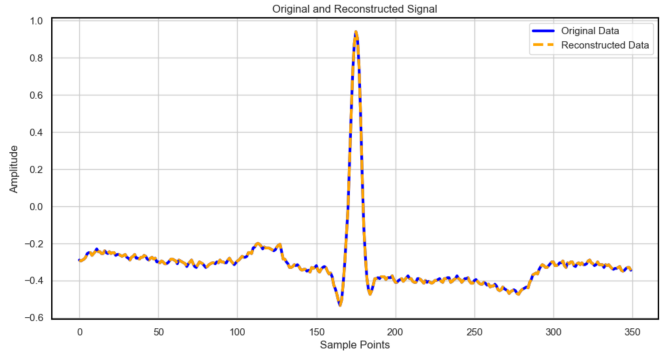

Figure 7. Comparison of original signal and reconstructed signal.

singular values shown in Figure 6. These modes effectively reflect the key dynamic features in the ECG signals, which helps in the subsequent analysis and classification tasks. With this approach, we are able to balance computational complexity with information retention, ensuring that the model avoids over-complexity while capturing the major modes in the data. At the 28th singular value a 90% course ratio is achieved, so that the extracted modal vectors are 28, providing a more comprehensive capture of the data trends.

These modes can better capture the dynamic features in the signal. To verify the effectiveness of the extracted modes, we reconstructed the original signal and compared it with the actual signal. Figure 7 demonstrates the effect of hankel DMD on the reconstructed signal on heart beat length of 351 data. It can be observed that the reconstructed signal is highly consistent with the original signal in terms of overall trend and shape, which verifies the effectiveness of the adopted signal processing and HDMD reconstruction methods. Especially in the main feature region of heartbeat, the reconstructed signal successfully captures the key dynamic changes of the original signal, indicating that the selected delay parameters and modal numbers can accurately recover the main information of the signal. Meanwhile, this reconstruction effectively reduces the noise and redundant information, making the main features of the signal clearer. It is further shown that Hankel DMD is able to extract more modes and achieve high-precision reproduction of complex signals.

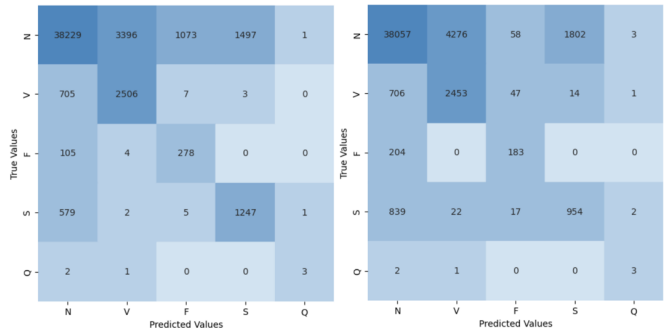

(a) HDMD-LSTM (b)LSTM

Figure 8. Confusion Matrix Heat Map for 2 Models.

4.3. *Analysis of classification results*

In order to validate the effectiveness of HDMD in ECG signal classification, two experimental protocols were designed and applied to the MIT-BIH arrhythmia five classification task in this study. First, the preprocessed ECG data were directly classified using a standard LSTM model. Then, in the second scheme, dynamic modal features of ECG signals are extracted using the HDMD method and these features are used as inputs to the LSTM for the same classification task. By comparing the performance of these two methods in terms of accuracy, precision, recall and F1 score, this study evaluates the role of HDMD in improving the classification performance of ECG signals and verifies its effectiveness in extracting dynamic features.

To evaluate the performance of different models in the arrhythmia classification task, the heatmap of the confusion matrix of HDMD + LSTM and directly using LSTM were plotted separately, as shown in Figure 8. When comparing the confusion matrices of HDMD + LSTM and LSTM alone models, the improvement in overall classification performance of HDMD + LSTM can be clearly seen. Firstly, the HDMD + LSTM model performs particularly well in the classification of S and F classes. In the classification of class S, HDMD + LSTM correctly classified 278 samples, while LSTM only classified 183, showing a significant advantage of HDMD + LSTM for this arrhythmia.The performance gap is also present in class F, where HDMD + LSTM correctly identified 1,247 samples, while LSTM only identified 954. HDMD + LSTM has significantly reduced misclassification on these two categories significantly reduces misclassification and improves the overall classification performance. Although the performance of the two models is relatively close in the classification of the N category, HDMD+LSTM has fewer misclassifications (3,396) than the LSTM model (4,276), showing a slight improvement in its accuracy when dealing with normal heart beats. In summary, the HDMD+LSTM model significantly improves the recognition of certain complex heartbeat categories (e.g., S and F categories) in the multi-classification task, indicating that the HDMD combined with LSTM approach can capture dynamic features more effectively and improve classification performance.

In order to visualise the results, the accuracy A, precision P, recall R, and F1 score of the five types of arrhythmias, namely,

Table 4. Classification results for different models.

Class	Model	A	P	R	F1
N	LSTM	0.70	0.94	0.70	0.80
	HDMD+LSTM	0.86	0.96	0.86	0.91
V	LSTM	0.64	0.22	0.64	0.33
	HDMD+LSTM	0.78	0.42	0.78	0.55
F	LSTM	0.58	0.05	0.58	0.10
	HDMD+LSTM	0.72	0.20	0.72	0.32
S	LSTM	0.52	0.31	0.52	0.38
	HDMD+LSTM	0.68	0.45	0.68	0.54
Q	LSTM	0.33	0.22	0.33	0.27
	HDMD+LSTM	0.50	0.60	0.50	0.55

N, V, F, S, and Q, were calculated according to the confusion matrices in Figures 8, respectively, as shown in Table 4:

In terms of these four metrics, the HDMD+LSTM model outperforms the LSTM model alone in overall performance, as shown in Table 4, especially in classifying more complex categories. In categories V and S, the HDMD+LSTM model shows significant improvement in accuracy and F1 score, indicating that the model is more accurate and less misclassified on these categories. And in class F, although the precision rate of HDMD+LSTM decreases, the recall rate is higher, indicating that it captures more samples in class F. Overall, HDMD+LSTM performs better in dealing with the more complex arrhythmia categories.

In addition, in Figure 9, two important metrics during model training are demonstrated: Figure 9 (a) shows the variation of training and testing losses with the number of training rounds. It can be seen that the training loss gradually decreases throughout the training process, while the testing loss shows the same decreasing trend at the beginning of training, but stabilises after reaching a certain number of training rounds. According to the early stopping mechanism, training stops when the validation loss does not decrease any more in 5 consecutive epochs. The results show that the model's validation set performance stabilises at the 36th epoch, and the validation loss no longer decreases significantly, which indicates that this number of epochs effectively ensures sufficient learning of model features and avoids overfitting. Figure 9 (b), on the other hand, demonstrates the variation of training and testing accuracy. According to this figure, the overall accuracy of the model reaches 0.851, reflecting excellent classification performance on all categories. The curves of both training and testing accuracy show that the classification performance of the model remains stable on both training and testing data, further validating the good performance of the model.

5. Discussion

Although the overall accuracy of the model is 81.5%, its greatest strength is its enhanced interpretability for modal extraction. Unlike other 'black box' models based on deep learning, the mathematical foundation of the Hankel DMD provides greater explanatory clarity. This is particularly important in the medical field, where doctors not only need to rely on the accuracy of the model, but also need to understand the basis of the model's decisions. With the dynamic modalities extracted by Hankel DMD, physicians can more intuitively identify the key factors affecting arrhythmia classification, thus enhancing the confidence of the clinical application. Although the overall classification accuracy did not reach the highest level expected, the significant performance in specific categories (e.g., normal beats) further validates the potential of the method for practical application.

Compared with other studies, the method proposed in this study demonstrated significant advantages in several aspects. For example, Fu *et al.* [32] achieved an accuracy of 62.94% in the 6-classification task of arrhythmia, which is significantly lower than the model proposed in this study. Hu *et al.* [33] achieved an accuracy of 76.58% in the 3-classification task, which fails to exceed the 81.5% accuracy obtained in the 5-classification task in this paper despite the lower difficulty of the task. The study by Guo *et al.* [34] achieved an accuracy of 75.33% in the 5-classification task, while the model in this paper demonstrated better classification performance. in which the accuracy was 75.33%, while the model in this paper showed better classification performance. In terms of F1 scores, the highest F1 score in this study reaches 0.91, which is a clear advantage over other multicategorisation studies. Gan *et al.* [35] study has an F1 score of 63.49 in the six-categorisation task, while Chen *et al.* [36] five-categorisation F1 score is 77.84, which is lower than the best F1 score in this paper. In addition, Essa *et al.* [37] and Pokaprakarn *et al.* [30] had F1 scores of 71.06 and 75.5 in the multi-classification task, respectively, neither of which exceeded the performance of the HDMD+LSTM method proposed in this paper. Although the F1 score of Xie *et al.* [38] is 88, which is close to the model in this paper, it still does not reach the highest score of 0.91. On the other hand, Zhu *et al.* [39] obtained an F1 score of 90.2 in the simpler binary classification task, however, due to the relative simplicity of the binary classification task, it cannot be directly compared with the five-classification results in this paper. Even so, the method proposed in this paper was able to maintain a high level of classification performance and F1 scores in the more complex five-classification task, reflecting its strong ability in complex arrhythmia classification tasks. In addition, Ran *et al.* [40] had an F1 score of 84.2 for a 6-classification study, whereas He *et al.* [41] had an F1 score of 84 for a 5-classification task, neither of which exceeded the maximum F1 score of 0.91, although they were close to the method in this paper.

In summary, the Hankel DMD combined with the LSTM model proposed in this paper demonstrates excellent performance in the five classification task of the MIT-BIH arrhythmia database, especially when dealing with complex arrhythmia types. Compared with other studies, this method not only excels in classification accuracy, but also provides higher interpretability and classification efficiency through modal extraction with Hankel DMD. In addition, the model combining HDMD and LSTM effectively reduces the input dimension of LSTM, decreases the computational complexity, and accelerates the convergence speed of the model. This combined strat-

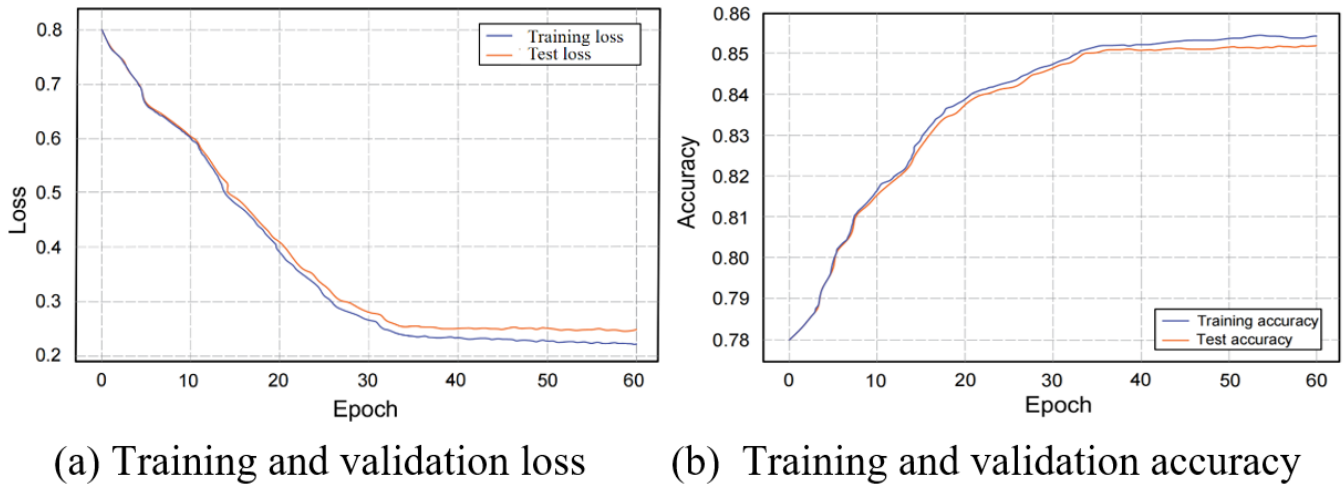

Figure 9. Loss and accuracy changes during model training.

egy achieved an average accuracy of 0.815 in the experiments, demonstrating the significant advantages and application potential of this method in arrhythmia multiclassification tasks.

6. Conclusion

In this paper, we propose an innovative model that combines HDMD and LSTM specifically for the task of multi-classification of cardiac arrhythmias and has been validated against the MIT-BIH arrhythmia database. The key innovation of the model is the use of 28 dynamic modal features extracted by HDMD as inputs to LSTM, which significantly improves the ability of LSTM to capture dynamic features of complex ECG signals. The experimental results show that HDMD-LSTM performs best in the classification of normal beats (N), with an F1 score of 0.91, an accuracy of 0.96, and an overall classification accuracy of 0.851. This approach effectively copes with the complexity in the classification of ECG signals, and provides a new perspective for the automated diagnosis of cardiac arrhythmias. Despite the excellent performance of HDMD-LSTM, it is still necessary to further explore how to solve the category imbalance problem and optimise the combination of DMD and LSTM to improve the feature extraction and classification performance. Overall, HDMD-LSTM provides new ideas and methods for the automated diagnosis of cardiac arrhythmias, demonstrating significant application potential and clinical value.

Acknowledgment

The authors are grateful to the "Ministry of higher education Malaysia for the fundamental research grant scheme" with Project Code: FRGS/1/2024/STG06/UMS/01/1 for their support in this research.

Data availability

The link to the dataset used in this study is provided here: https://physionet.org/content/mitdb/.

References

[1] C. Antzelevitch & A. Burashnikov, "Overview of basic mechanisms of cardiac arrhythmia", Cardiac Electrophysiology Clinics **3** (2011) 23. https://doi.org/10.1016/j.ccep.2010.10.012.

[2] R. Gopinathannair, S. P. Etheridge, F. E. Marchlinski, F. G. Spinale, D. Lakkireddy & B. Olshansky, "Arrhythmia-induced cardiomyopathies: mechanisms, recognition, and management", Journal of the American College of Cardiology **66** (2015) 1714. https://doi.org/10.1016/j.jacc.2015.08.038.

[3] M. Saber & M. Abotaleb, "Arrhythmia modern classification techniques: A review", Journal of Artificial Intelligence and Metaheuristics **1** (2022) 42. https://doi.org/10.54216/JAIM.010205.

[4] P. J. Schmid, "Dynamic mode decomposition and its variants", Annual Review of Fluid Mechanics **54** (2022) 225. https://doi.org/10.1146/annurev-fluid-030121-015835.

[5] H. N. Ingabire, K. Wu, J. T. Amos, S. He, X. Peng, W. Wang & P. Ren, "Analysis of ECG signals by dynamic mode decomposition", IEEE Journal of Biomedical and Health Informatics **26** (2021) 2124. https://doi.org/10.1109/JBHI.2021.3130275.

[6] Y. Yu, X. Si, C. Hu & J. Zhang, "A review of recurrent neural networks: LSTM cells and network architectures", Neural Computation **31** (2019) 1235. https://doi.org/10.1162/neco_a_01199.

[7] M. G. Tsipouras, D. I. Fotiadis & D. Sideris, "An arrhythmia classification system based on the RR-interval signal", Artificial Intelligence in Medicine **33** (2005) 237. https://doi.org/10.1016/j.artmed.2004.03.007.

[8] Y. Kutlu, G. Altan & N. Allahverdi, "Arrhythmia classification using waveform ECG signals", presented at International Conference on Advanced Technology & Sciences, Konya, Turkey, 2016. https://www.researchgate.net/publication/308919881_Arrhythmia_Classification_Using_Waveform_ECG_Signals

[9] J. A. Nasiri, M. Naghibzadeh, H. S. Yazdi & B. Naghibzadeh, "ECG arrhythmia classification with support vector machines and genetic algorithm", Proceedings of the 2009 Third UKSim European Symposium on Computer Modeling and Simulation, 2009, pp. 187–192. https://doi.org/10.1109/EMS.2009.39.

[10] B. M. Asl, S. K. Setarehdan & M. Mohebbi, "Support vector machine-based arrhythmia classification using reduced features of heart rate variability signal", Artificial Intelligence in Medicine **44** (2008) 51. https://doi.org/10.1016/j.artmed.2008.04.007.

[11] W. H. Jung and S. G. Lee, "An arrhythmia classification method utilizing the weighted KNN and the fitness rule", IRBM **38** (2017) 138. https://doi.org/10.1016/j.irbm.2017.04.002.

[12] W. M. Zuo, W. G. Lu, K. Q. Wang & H. Zhang, "Diagnosis of cardiac arrhythmia using kernel difference weighted KNN classifier", 2008 Computers in Cardiology (2008) 253. https://doi.org/10.1109/CIC.2008.4749025.

[13] R. Kumari Mohebbanaaz, L. V. Rajani & Y. Padma Sai, "Classification of arrhythmia beats using optimized K-nearest neighbor classifier", Intelligent Systems: Proceedings of ICMIB, Springer Singapore, 2020, pp. 349—359. https://doi.org/10.1007/978-981-33-6081-5_31.

[14] Z. Ebrahimi, M. Loni, M. Daneshtalab & A. Gharehbaghi, "A review on deep learning methods for ECG arrhythmia classification", Expert Systems with Applications **7** (2020) 100033. https://doi.org/10.1016/j.eswax.2020.100033.

[15] C. Chen, Z. Hua, R. Zhang, G. Liu & W. Wen, "Automated arrhythmia classification based on a combination network of CNN and LSTM", Biomedical Signal Processing and Control **57** (2020) 101819. https://doi.org/10.1016/j.bspc.2019.101819.

[16] T. J. Jun, H. M. Nguyen, D. Kang, D. Kim, D. Kim & Y. H. Kim, "ECG arrhythmia classification using a 2-D convolutional neural network", arXiv preprint (2018). https://www.semanticscholar.org/paper/ECG-arrhythmia-classification-using-a-2-D-neural-Jun-Nguyen/622d18e3622f05bfe2054703318ea71747975dd0.

[17] M. Salem, S. Taheri & J. S. Yuan, "ECG arrhythmia classification using transfer learning from 2-dimensional deep CNN features", presented at the 2018 IEEE Biomedical Circuits and Systems Conference , Cleveland, OH, USA, 2018, pp. 1–4. https://doi.org/10.1109/BIOCAS.2018.8584808.

[18] B. Hou, J. Yang, P. Wang & R. Yan, "LSTM-based auto-encoder model for ECG arrhythmias classification", IEEE Transactions on Instrumentation and Measurement **69** (2019) 1232. https://doi.org/10.1109/TIM.2019.2910342.

[19] P. Liu, X. Sun, Y. Han, Z. He, W. Zhang & C. Wu, "Arrhythmia classification of LSTM autoencoder based on time series anomaly detection", Biomedical Signal Processing and Control **71** (2022) 103228. https://doi.org/10.1016/j.bspc.2021.103228.

[20] C. Chen, Z. Hua, R. Zhang, G. Liu & W. Wen, "Automated arrhythmia classification based on a combination network of CNN and LSTM", Biomedical Signal Processing and Control **57** (2020) 101819. https://doi.org/10.1016/j.bspc.2019.101819.

[21] R. He, Y. Liu, K. Wang, N. Zhao, Y. Yuan, Q. Li & H. Zhang, "Automatic cardiac arrhythmia classification using combination of deep residual network and bidirectional LSTM", IEEE Access **7** (2019) 102119. https://doi.org/10.1109/ACCESS.2019.2931500.

[22] E. Vasconcelos Filho and P. L. dos Santos, "A dynamic mode decomposition approach with Hankel blocks to forecast multi-channel temporal series", IEEE Control Systems Letters **3** (2019) 739. https://doi.org/10.1109/LCSYS.2019.2917811.

[23] J. H. Tu, Dynamic mode decomposition: Theory and applications, Ph.D. dissertation, Princeton University, 2013. https://robotics.caltech.edu/wiki/images/c/c7/DMDApplicationsTheory.pdf.

[24] J. Chung, C. Gulcehre, K. Cho & Y. Bengio, "Empirical evaluation of gated recurrent neural networks on sequence modeling", arXiv preprint, arXiv:1412.3555 (2014). https://arxiv.org/abs/1412.3555.

[25] Y. LeCun, Y. Bengio & G. Hinton, "Deep learning", Nature **521** (2015) 436. https://doi.org/10.1038/nature14539.

[26] A. Goldberger, L. Amaral, L. Glass, J. Hausdorff, P. C. Ivanov, R. Mark & H. E. Stanley, "PhysioBank, PhysioToolkit, and PhysioNet: Components of a new research resource for complex physiologic signals", Circulation **101** (2000) e215. https://doi.org/10.1161/01.CIR.101.23.e215.

[27] B. Zhao, H. Liu, T. Bi & S. Xu, "Synchrophasor measurement method based on cascaded infinite impulse response and dual finite impulse response filters", Journal of Modern Power Systems and Clean Energy (2024). https://doi.org/10.35833/MPCE.2023.000824.

[28] F. Mumtaz, T. S. Khan, M. Alqahtani, H. A. Sher, A. S. Aljumah & S. Z. Almutairi, "Ultra high-speed fault diagnosis scheme for DC distribution systems based on discrete median filter and mathematical morphology", IEEE Access (2024). https://doi.org/10.1109/ACCESS.2024.3381519.

[29] P. De Chazal, *Detection of supraventricular and ventricular ectopic beats using a single lead ECG*, Proceedings of the 2013 35th Annual International Conference of the IEEE Engineering in Medicine and Biology Society (EMBC), IEEE, 2013, pp. 45–48. https://doi.org/10.1109/EMBC.2013.6609433.

[30] T. Pokaprakarn, R. R. Kitzmiller, J. R. Moorman, D. E. Lake, A. K. Krishnamurthy & M. R. Kosorok, "Sequence to sequence ECG cardiac rhythm classification using convolutional recurrent neural networks", IEEE Journal of Biomedical and Health Informatics **26** (2021) 572. https://doi.org/10.1109/JBHI.2021.3098662.

[31] X. Wang & L. Sun, "Extracting dynamic mobility patterns by Hankel dynamic modes decomposition", presented at The 11th Triennial Symposium on Transportation Analysis, Mauritius Island, Apr. 2022.

[32] L. Fu, B. Lu, B. Nie, Z. Peng, H. Liu & X. Pi, "Hybrid network with attention mechanism for detection and location of myocardial infarction based on 12-lead electrocardiogram signals", Sensors **20** (2020) 1020. https://doi.org/10.3390/s20041020.

[33] J. Hu, W. Zhao, D. Jia, C. Yan, H. Wang, Z. Li, J. Fang & M. Yang, "Deep multi-instance networks for bundle branch block detection from multi-lead ECG", in Proc. 2020 42nd Annu. Int. Conf. IEEE Eng. Med. Biol. Soc. (EMBC), 2020, pp. 20–24. https://doi.org/10.1109/EMBC44109.2020.9175909.

[34] L. Guo, G. Sim & B. Matuszewski, "Inter-patient ECG classification with convolutional and recurrent neural networks", Biocybernetics and Biomedical Engineering **39** (2019) 868. https://doi.org/10.1016/j.bbe.2019.06.001.

[35] Y. Gan, J. C. Shi, W. M. He & F. J. Sun, "Parallel classification model of arrhythmia based on DenseNet-BiLSTM", Biocybernetics and Biomedical Engineering **41** (2021) 1548. https://doi.org/10.1016/j.bbe.2021.09.001.

[36] A. Chen, F. Wang, W. Liu, S. Chang, H. Wang, J. He & Q. Huang, "Multi-information fusion neural networks for arrhythmia automatic detection", Comput. Methods Programs Biomed **193** (2020) 105479. https://doi.org/10.1016/j.cmpb.2020.105479.

[37] E. Essa and X. Xie, "An ensemble of deep learning-based multi-model for ECG heartbeats arrhythmia classification", IEEE Access **9** (2021) 103452. https://doi.org/10.1109/ACCESS.2021.3098986.

[38] Q. Xie, S. Tu, G. Wang, Y. Lian & L. Xu, "Feature enrichment based convolutional neural network for heartbeat classification from electrocardiogram", IEEE Access **7** (2019) 153751. https://doi.org/10.1109/ACCESS.2019.2948857.

[39] J. Zhu, J. Lv & D. Kong, "CNN-FWS: A model for the diagnosis of normal and abnormal ECG with feature adaptive", Entropy **24** (2022) 471. https://doi.org/10.3390/e24040471.

[40] S. Ran, X. Yang, M. Liu, Y. Zhang, C. Cheng, H. Zhu & Y. Yuan, "Homecare-oriented ECG diagnosis with large-scale deep neural network for continuous monitoring on embedded devices", IEEE Transactions on Instrumentation and Measurement **71** (2022) 1. https://doi.org/10.1109/TIM.2022.3147328.

[41] J. He, J. Rong, L. Sun, H. Wang & Y. Zhang, "An advanced two-step DNN-based framework for arrhythmia detection", in *Advances in Knowledge Discovery and Data Mining*, Springer International Publishing, 2020, pp. 422–434. https://doi.org/10.1007/978-3-030-47436-2_32.